



University of Pennsylvania
ScholarlyCommons

Departmental Papers (MSE)

Department of Materials Science & Engineering

February 2005

Optical evidence for transient photoinduced magnetization in $\text{La}_{0.7}\text{Ca}_{0.3}\text{MnO}_3$

S. A. McGill
University of Pennsylvania

R. I. Miller
University of Pennsylvania

O. N. Torrens
University of Pennsylvania

Alexander Mamchik
University of Pennsylvania

I-Wei Chen
University of Pennsylvania, iweichen@seas.upenn.edu

See next page for additional authors

Follow this and additional works at: http://repository.upenn.edu/mse_papers

Recommended Citation

McGill, S. A., Miller, R. I., Torrens, O. N., Mamchik, A., Chen, I., & Kikkawa, J. M. (2005). Optical evidence for transient photoinduced magnetization in $\text{La}_{0.7}\text{Ca}_{0.3}\text{MnO}_3$. Retrieved from http://repository.upenn.edu/mse_papers/70

Copyright American Physical Society. Reprinted from *Physical Review B*, Volume 71, Issue 7, Article 075117, February 2005, 5 pages.
Publisher URL: <http://dx.doi.org/10.1103/PhysRevB.71.075117>

This paper is posted at ScholarlyCommons. http://repository.upenn.edu/mse_papers/70
For more information, please contact libraryrepository@pobox.upenn.edu.

Optical evidence for transient photoinduced magnetization in $\text{La}_{0.7}\text{Ca}_{0.3}\text{MnO}_3$

Abstract

Pump-probe Kerr spectroscopy reveals evidence for transient photoinduced magnetization (PIM) near T_c in the colossally magnetoresistive manganite $\text{La}_{0.7}\text{Ca}_{0.3}\text{MnO}_3$. For temperatures above T_c , the PIM signature reaches full strength at the field-driven magnetic phase transition, while below T_c it exhibits a magnetic activation threshold of ~ 0.5 T. We compare the temperature dependence of the effect with diffuse spin scattering previously measured with neutrons and discuss these findings in the context of phase separation near T_c .

Comments

Copyright American Physical Society. Reprinted from *Physical Review B*, Volume 71, Issue 7, Article 075117, February 2005, 5 pages.

Publisher URL: <http://dx.doi.org/10.1103/PhysRevB.71.075117>

Author(s)

S. A. McGill, R. I. Miller, O. N. Torrens, Alexander Mamchik, I-Wei Chen, and J. M. Kikkawa

Optical evidence for transient photoinduced magnetization in $\text{La}_{0.7}\text{Ca}_{0.3}\text{MnO}_3$

S. A. McGill,¹ R. I. Miller,¹ O. N. Torrens,¹ A. Mamchik,² I-Wei Chen,² and J. M. Kikkawa¹

¹Department of Physics and Astronomy, University of Pennsylvania, Philadelphia, Pennsylvania 19104, USA

²Department of Materials Science & Engineering, University of Pennsylvania, Philadelphia, Pennsylvania 19104, USA

(Received 23 April 2004; revised manuscript received 19 August 2004; published 24 February 2005)

Pump-probe Kerr spectroscopy reveals evidence for transient photoinduced magnetization (PIM) near T_c in the colossally magnetoresistive manganite $\text{La}_{0.7}\text{Ca}_{0.3}\text{MnO}_3$. For temperatures above T_c , the PIM signature reaches full strength at the field-driven magnetic phase transition, while below T_c it exhibits a magnetic activation threshold of ~ 0.5 T. We compare the temperature dependence of the effect with diffuse spin scattering previously measured with neutrons and discuss these findings in the context of phase separation near T_c .

DOI: 10.1103/PhysRevB.71.075117

PACS number(s): 75.47.Lx, 71.30.+h, 72.25.Rb, 78.20.Ls

The colossally magnetoresistive (CMR) manganites continue to challenge our understanding of strongly correlated systems. Phase separation is observed on a variety of length scales in these materials and appears central to our understanding of their complex insulator-metal (IM) transitions.^{1,2} CMR manganites are also optically responsive, and pump-probe methods may provide a uniquely comprehensive picture of locally pump-induced phase transitions from the individual perspectives of the spin, charge, and lattice degrees of freedom. Pump pulses may initiate phase separation, encouraging local IM transitions,³ changes in charge order,^{3,4} and spin disordering.^{5,6} When such changes are *reversible*, monitoring the breakdown and restoration of magnetic and charge states could eventually yield spatial information about phase-separation dynamics.

Previously, we showed in the manganites that time-resolved Kerr effects can measure transient magnetization dynamics and that this method is highly sensitive to the presence of magnetic phase separation.⁵ In this study, these techniques reveal two-component Kerr responses in $\text{La}_{0.7}\text{Ca}_{0.3}\text{MnO}_3$ (LCMO) near T_c , where other methods have identified phase separation into paramagnetic (PM) and ferromagnetic (FM) regions.⁷⁻¹¹ A fast Kerr transient arises from pump-induced demagnetization (PID) and is present well below T_c . The slower component appears only in the vicinity of the field-driven IM and magnetic phase transitions and is most likely due to a process of pump-induced magnetization (PIM). Previous studies have reported PIM in dilute magnetic semiconductors, attributed to the proliferation of magnetic polarons.¹² Yet CMR manganites feature strong coupling between carrier density and magnetic order, and their phase instabilities demonstrate that competing states are close in energy over a wide range of external parameters. These systems are therefore strong candidates for transient (i.e., *reversible*) photonucleation of magnetic order. Comparisons of our Kerr data to neutron-scattering measurements indicate that phase separation may play an important role in the nucleation of PIM.

Preparation of the bulk $\text{La}_{0.7}\text{Ca}_{0.3}\text{MnO}_3$ samples studied here is described elsewhere.⁵ Routine sample characterization includes electrical resistivity, dc magnetization ($T_c = 255$ K), ac magnetic susceptibility, and dc polar Kerr effect

measurements performed from 5 to 300 K and at magnetic fields up to 9 T. Simultaneous transient polar Kerr and reflectivity studies are performed with subpicosecond resolution as described elsewhere.^{5,13} In dc Kerr studies, we employ a specially modified cryostat for which window contributions are below our measurement noise. In all time-resolved measurements, the pump is linearly polarized. Importantly, we employ a field-pairing method for both dc and time-resolved Kerr effects that isolates responses that are odd under sign reversal of the field direction and history.⁵ For example, the transient rotation is obtained by subtracting measurements taken at opposite magnetic fields and sweep directions and is reported as $\Delta\theta(B) \equiv [\Delta\theta^{inc}(B) - \Delta\theta^{dec}(-B)]/2$. In this expression, $\Delta\theta^{inc}$ and $\Delta\theta^{dec}$ are transient rotations obtained during increasing and decreasing field sweeps, respectively. The same method is used to obtain the transient ellipticity, $\Delta\eta$, as well as the dc Kerr signals, θ and η . To maintain a consistent sample history, the magnetic-field sweep rate (0.5 T/min) and measurement times for *all* data collections are computer controlled and identical.

To linear order, θ and η are written as $\theta = f \cdot M$ and $\eta = g \cdot M$, where f and g are magneto-optical (M-O) couplings and M is the magnetization. In conventional ferromagnets, the classic application of the Kerr effect is to extract $M(B)$ from a Kerr hysteresis loop. In the manganites, however, field-induced IM transitions give rise to a redistribution of optical spectral weight that generally changes both f and g .^{5,6} Hence, the correspondence between $\theta(B)$ [or $\eta(B)$] and $M(B)$ cannot be taken for granted.¹⁴ In pump-probe studies of the manganites one further encounters *dynamic* spectral weight shifts,¹⁵ which may induce dynamics in f and g . Here, we study the dc Kerr effect to assess the reliability of subsequent time-resolved measurements in capturing magnetization dynamics. In LCMO, a static magnetic field can produce optical spectral weight shifts much larger than those induced in our time-resolved measurements by the pump pulse. So by studying the fidelity of the dc Kerr effects in mapping out $M(B)$, M-O artifacts are revealed and can be minimized by proper choice of optical energy.

Figures 1(a) and 1(b) compare the profiles of θ and η at 1.55 eV for temperatures just below and above T_c , respectively. The data for $\eta(B)$ show a strong departure from $M(B)$

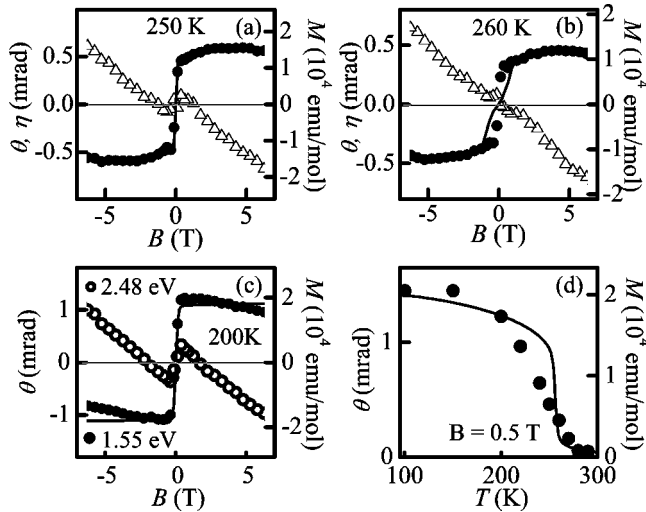


FIG. 1. dc Kerr rotation (θ , solid circles), ellipticity (η , open triangles), and magnetization (M , solid line) vs magnetic field at (a) $T=250$ K and (b) $T=260$ K. (c) $\theta(B)$ for 1.55 eV (solid circles) and 2.48 eV (open circles) are compared to $M(B)$ (solid line) at $T=200$ K. (d) θ at 1.55 eV (solid circles) and M (solid line) vs T at a fixed field $B=0.5$ T.

(solid line) that results from spectral weight transfer. Although this behavior is typical of η and θ for most energies, we find that at 1.55 eV $\theta(B)$ is a comparatively good measure of $M(B)$. The temperatures shown in Figs. 1(a) and 1(b) are chosen to highlight a difference between $\theta(B)$ and $M(B)$ which does, however, arise near T_c . In comparing data just below and above the bulk T_c , the initial slope of $M(B)$ softens above T_c whereas $\theta(B)$ remains largely unchanged. We believe the latter reflects an elevated surface T_c , as observed in similarly prepared CMR samples,⁵ although additional M-O contributions cannot be ruled out. Note that the accuracy of rotation in measuring the magnetization is lost for energies away from 1.55 eV [Fig. 1(c)].

The data of Figs. 1(a)–1(c) indicate that at 1.55 eV the M-O coupling f is relatively constant across field sweeps at a fixed temperature. This behavior demonstrates a resilience of f at 1.55 eV to spectral weight shifts induced by the magnetic field, which are large in this system and produce dramatic changes in g (and in f at other energies). The existence of special energies for which either θ or η decouple from M-O artifacts has been previously discussed,^{6,16} and our data indicate that θ at 1.55 eV is fairly well isolated from such changes and constitutes a good choice of probe energy for time-resolved studies. A temperature dependence of θ and M at $B=0.5$ T [Fig. 1(d)] shows there is indeed some change in f with temperature. With these observations in mind, in what follows we present $\Delta\theta$ as a *qualitative* probe of the magnetization dynamics in the system and consider that a M-O coupling transient (i.e., $\Delta f \cdot M$) may also contribute to the observed signal.

Magnetic-field scans taken at a fixed time delay can greatly facilitate the interpretation of time-resolved data on magnetic systems. Consider, for example, the limit in which M is saturated prior to the pump arrival ($T \ll T_c$). In this case, the pump generally induces spin disorder and a net reduction

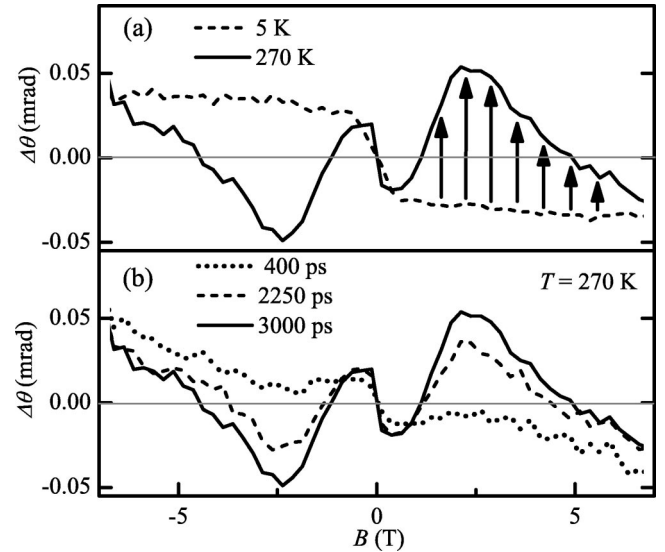


FIG. 2. (a) Transient Kerr rotation, $\Delta\theta(B)$, at $T=5$ K (dashed line) and $T=270$ K (solid line) for a fixed time delay $\Delta t=3000$ ps. (b) $\Delta\theta(B)$ at $T=270$ K for various Δt showing the gradual evolution of the PIM rotation peak.

in magnetization, $\Delta M/M < 0$; and as M reorients in a changing magnetic field, ΔM responds with a characteristic profile that is proportional to M and of opposite sign. Figure 2(a) confirms that this signature of PID appears in field scans of $\Delta\theta$ at $T=5$ K, where $\Delta\theta$ reproduces the low-temperature behavior of M [Fig. 1(c)].

Close to and above T_c , however, dramatic changes in the $\Delta\theta(B)$ profile suggest a sign reversal of ΔM relative to PID. Instead of scaling with $-M$, $\Delta\theta$ at $T=270$ K [Fig. 2(a)] changes sign and reaches an additional maximum at a field we denote B_θ . Moving away from $B_\theta=2.4$ T toward higher field strengths, the transient signal becomes consistent with PID again. A purely magnetic interpretation of $\Delta\theta$ (where a transient in f is ignored) would indicate that above T_c pump-induced magnetization processes coexist with or replace PID whenever B is close to B_θ . Note that the persistence of some PID processes above T_c is consistent with the suggestion from dc Kerr data that the surface T_c is higher than in the bulk [Fig. 1(b)]. The arrows in Fig. 2(a) illustrate an interpretation in which PIM is superimposed on a background of PID (we refer to this former feature as the ‘‘PIM rotation peak’’).

The coexistence of PIM and PID processes, even at the maximum of the PIM rotation peak, is established by their time evolution. We observe a two-component temporal response, with a faster component associated with PID and a slower component corresponding to the PIM rotation peak. This behavior is most clearly resolved in field sweeps of $\Delta\theta$ taken at different time delays at $T=270$ K. Such scans are shown in Fig. 2(b), where it can be seen that PID is established across the entire field range by $\Delta t=400$ ps, creating a baseline from which the PIM rotation peak grows on a nanosecond time scale. Time delay scans at fixed fields (Fig. 3) show this superposition with better time resolution. At $B=1.5$ T, near B_θ , $\Delta\theta$ comprises an initial negative signal (associated with PID) that rises over several hundred picosec-

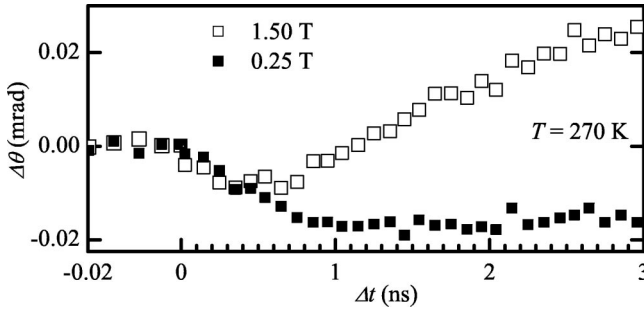


FIG. 3. $\Delta\theta$ at $B=0.25$ T (solid), and $B=1.5$ T (open). Data taken at $T=270$ K.

onds and a large positive signal (the PIM rotation peak) that develops more slowly over a few nanoseconds. As one moves away from B_θ , the latter component vanishes. For example, no positive component is seen at $B=0.25$ T, where PID dominates.

If the PIM rotation peak is magnetic in origin, then one might expect it to occur under conditions of greatest magnetic instability. Note that the pump pulse carries no angular momentum in our experiment, and that the applied field breaks the symmetry for PIM. In LCMO, a PM-to-FM transition can be induced by a magnetic field for temperatures close to but above T_c , resulting in peaks in the ac magnetic susceptibility, χ' , at the magnetic critical field strength, B_χ . A comparison of χ' and $\Delta\theta$ [Figs. 4(a) and 4(b), respectively] shows that above T_c the PIM rotation peak is correlated with magnetic instability ($B_\theta \approx B_\chi$). At T_c and below, however, the susceptibility maxima converge to a single zero-field peak while the PIM rotation peak remains at a finite field ($B_\theta \approx 0.5$ T) well below T_c [Fig. 4(c)]. The temperature dependence of B_θ and B_χ is summarized in Fig. 5(a), and strongly suggests a magnetic activation energy for, and a magnetic interpretation of, the PIM rotation peak.

As discussed above, transient changes in the M-O coupling constants can yield a transient Kerr effect even when ΔM is zero, so their contribution to the PIM rotation peak needs to be considered. The Kerr rotation transient in this case is given by $\Delta\theta = f \cdot \Delta M + \Delta f \cdot M$. As detailed in Refs. 5, 14, and 17–19, one normally uses measurements of $\Delta\eta$ to deduce the nonmagnetic M-O contribution to $\Delta\theta$, given by the second term in $\Delta\theta$ proportional to Δf . However, Figs. 1(a) and 1(b) show that $\Delta\eta$ is highly unreliable as a measure of ΔM . And since prior studies show that M-O coupling transients in LCMO persist beyond the time window of our experiment,⁵ magnetization transients cannot be identified unambiguously by performing both types of Kerr measurements.

Nonetheless, the behavior of the transient reflectivity can be used to explore the converse and help determine if the signal $\Delta\theta$ is purely nonmagnetic. Changes in the diagonal elements of the dielectric tensor ϵ strongly affect f ,^{5,6} and so Δf is expected to respond to transient changes in reflectivity, $\Delta R/R$. Figure 4(d) shows that above T_c , $\Delta R/R$ is strongly peaked at the dielectric critical field, B_ϵ , associated with the field-induced IM boundary. Numerous studies have shown that pump-induced shifts in optical spectral weight (“dynamic spectral weight transfer”) are largest at the IM

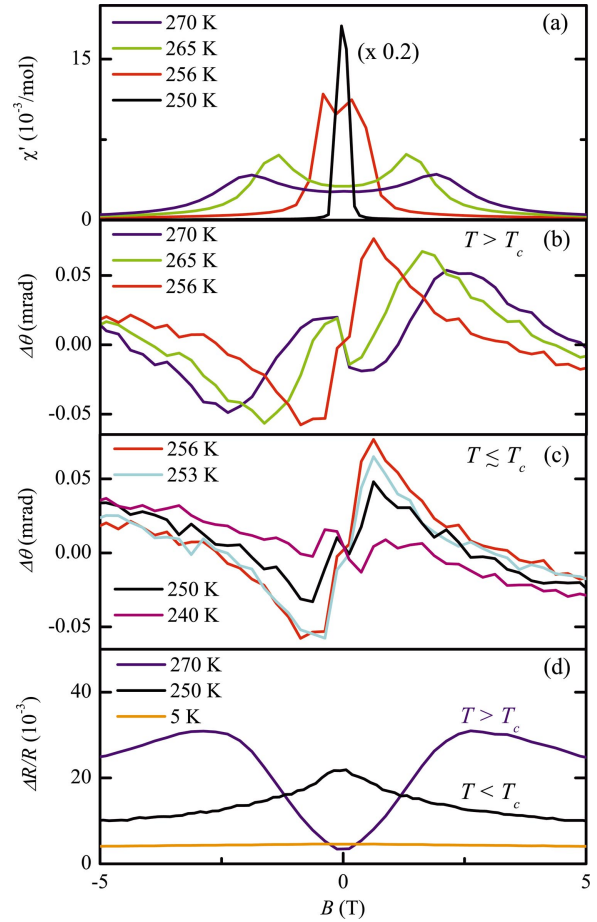


FIG. 4. (Color) (a) ac susceptibilities for the field-driven magnetic phase transition at various T . The data at $T=250$ K has been scaled by 0.2. (b) $\Delta\theta(B)$ at fixed $\Delta t=3000$ ps for $T > T_c$ and (c) $T \lesssim T_c$. Data at $T=256$ K is shown in both (b) and (c) for comparative purposes. (d) Transient reflectivity, $\Delta R/R$, at $\Delta t=3000$ ps for $T=270, 250$, and 5 K.

transition.^{4,15,20} Since the IM and PM-to-FM transitions coincide, similar behavior of B_ϵ and B_χ above T_c [Fig. 5(a)] is not surprising and one might then suppose that transient M-O artifacts account for the PIM rotation peak at B_θ . But the behavior below T_c makes such a nonmagnetic interpretation of the PIM rotation peak rather difficult. Note that $B_\epsilon \rightarrow 0$ at T_c . So below T_c , there are no transient reflectivity features at $B=0.5$ T which might explain the PIM rotation peak. In other words, the PIM rotation peak persists down to temperatures where the field-driven IM transition is no longer possible. These data show that a M-O coupling transient associated with $\Delta R/R$ does not account for the PIM rotation peaks seen below T_c , and strongly point to pump-induced magnetization as the origin of these features.

Since different physical processes such as PIM and PID can be distinguished by their temporal signatures, transient Kerr spectroscopy creates opportunities for exploring non-equilibrium dynamics of phase separation in the manganites. Interestingly, the temperature dependence of the PIM rotation peak is similar to that of short-range magnetic correlations near T_c , which have been measured by neutron scattering¹¹ and discussed within the context of phase separation.

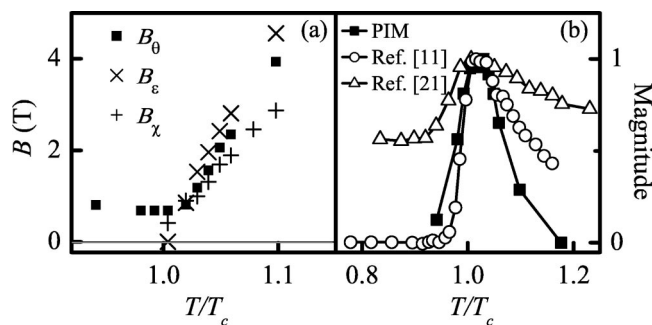


FIG. 5. (a) Critical fields B_0 , B_χ , and B_e , as defined in the text. (b) Magnitude of the QES amplitude in Ref. 11 (open circles) and correlated polaron amplitude in Ref. 21 (open triangles) compared with the PIM rotation peak amplitude in $\Delta\theta$ (solid squares). The neutron and optical data have been normalized to 1 at T_c for comparative purposes.

ration. This comparison appears in Fig. 5(b), where we plot the amplitude of the PIM rotation peak along with published neutron-scattering intensities and quasielastic scattering (QES) in the spin-fluctuation spectrum.¹¹ The QES component has been attributed to short-range spin diffusion on the Mn sublattice,¹⁰ and similar small-angle neutron-scattering (SANS) results have been interpreted as evidence for short-range ferromagnetic clusters around T_c .²²

Figure 5(b) shows these magnetic correlations appear simultaneously with an apparent instability toward magnetic ordering upon photoexcitation. Note that PIM is *transitory* and does not identify the type of magnetic fluctuations that may exist at *equilibrium* as observed in the QES and SANS data. With this in mind, our data suggest that the following possibilities merit further study: (1) The presence of FM clusters could be necessary for PIM, which encourages their enlargement and/or proliferation. The magnetic dynamics of photoinduced magnetic polarons have been observed in a rather different system, dilute magnetic semiconductors,¹² where polaron moments are thought to organize on a time

scale faster than spin-lattice relaxation through nonscalar spin-spin interactions.²³ Although the physics of $\text{La}_{0.7}\text{Ca}_{0.3}\text{MnO}_3$ is quite different, the onset of the PIM signal in our sample (Fig. 3) does fall in the range between spin-spin and spin-lattice relaxation times near the IM transition in LCMO, from 250 ps to a few nanoseconds, respectively.²⁴ (2) The PIM signal may instead represent a change in the volume fraction of competing FM and PM phases on a larger spatial length scale.¹ Though the comparison in Fig. 5(b) suggests a connection between our data and phase separation, quantities that peak around T_c are commonplace in the manganites, including anomalous volume expansion,²² carrier relaxation times,¹⁵ and the number of correlated lattice polarons^{11,21} [also shown in Fig. 5(b) for comparison]. While many of these phenomena are indeed interrelated,^{10,11,22,25,26} it is premature to draw a causal relationship between the observation of ferromagnetic clusters by neutron scattering and our Kerr data.

In conclusion, these studies provide intriguing signatures of pump-induced magnetization in $\text{La}_{0.7}\text{Ca}_{0.3}\text{MnO}_3$. A two-component response appears to result from simultaneous photoinduced spin disordering and photonucleated spin ordering near T_c . These findings contrast with numerous prior pump-probe optical studies of this system, in which charge dynamics near T_c in LCMO were interpreted entirely in the context of spin disordering.¹⁵ Future studies of PIM dynamics could lead to an improved understanding of phase separation near T_c , and may reveal coupled spin-charge modes whose temporal evolution could provide a direct measurement of spin-charge couplings in these systems.

Note added in proof. Related work on FeRh thin films was recently published by Ju *et al.*²⁷

We thank Valery Kiryukhin for helpful discussions. This work is supported by NSF-DMR-0094156, -0079909, and -0303458, DARPA under ONR Grant No. N00015-01-1-0831, the Sloan Foundation, and the Research Corporation.

¹M. Uehara, S. Mori, C. H. Chen, and S.-W. Cheong, *Nature* (London) **399**, 560 (1999).

²A. Moreo, S. Yunoki, and E. Dagotto, *Science* **283**, 2034 (1999); E. Dagotto, *Nanoscale Phase Separation and Colossal Magnetoresistance* (Springer-Verlag, Berlin, 2002).

³M. Fiebig, K. Miyano, Y. Tomioka, and Y. Tokura, *Appl. Phys. Lett.* **74**, 2310 (1999); M. Fiebig, K. Miyano, Y. Tomioka, and Y. Tokura, *Appl. Phys. B: Lasers Opt.* **B71**, 211 (2000).

⁴X. J. Liu, Y. Moritomo, A. Machida, A. Nakamura, H. Tanaka, and T. Kawai, *Phys. Rev. B* **63**, 115105 (2001).

⁵S. A. McGill, R. I. Miller, O. N. Torrens, A. Mamchik, I-Wei Chen, and J. M. Kikkawa, *Phys. Rev. Lett.* **93**, 047402 (2004).

⁶T. Ogasawara, M. Matsubara, Y. Tomioka, M. Kuwata-Gonokami, H. Okamoto, and Y. Tokura, *Phys. Rev. B* **68**, 180407(R) (2003).

⁷V. Chechersky, A. Nath, I. Isaac, J. P. Franck, K. Ghosh, H. Ju, and R. L. Greene, *Phys. Rev. B* **59**, 497 (1999); V. Chechersky,

A. Nath, I. Isaac, J. P. Franck, K. Ghosh, and R. L. Greene, *ibid.* **63**, 052411 (2001).

⁸R. H. Heffner, J. E. Sonier, D. E. MacLaughlin, G. J. Nieuwenhuys, G. Ehlers, F. Mezei, S.-W. Cheong, J. S. Gardner, and H. Röder, *Phys. Rev. Lett.* **85**, 3285 (2000).

⁹G. Li, S.-J. Feng, F. Liu, Y. Yang, R.-K. Zheng, T. Qian, X.-Y. Guo, and X.-G. Li, *Eur. Phys. J. B* **32**, 5 (2003).

¹⁰J. W. Lynn, R. W. Erwin, J. A. Borchers, Q. Huang, A. Santoro, J.-L. Peng, and Z. Y. Li, *Phys. Rev. Lett.* **76**, 4046 (1996); J. W. Lynn, R. W. Erwin, J. A. Borchers, A. Santoro, Q. Huang, J.-L. Peng, and R. L. Greene, *J. Appl. Phys.* **81**, 5488 (1997).

¹¹C. P. Adams, J. W. Lynn, Y. M. Mukovskii, A. A. Arsenov, and D. A. Shulyatev, *Phys. Rev. Lett.* **85**, 3954 (2000).

¹²D. D. Awschalom, J.-M. Halbout, S. von Molnár, T. Siegrist, and F. Holtzberg, *Phys. Rev. Lett.* **55**, 1128 (1985); D. D. Awschalom, J. Warnock, and S. von Molnár, *ibid.* **58**, 812 (1987).

- ¹³Time-resolved studies use 1-kHz pump and probe pulses at 3.1 eV ($260 \mu\text{J}/\text{cm}^2/\text{pulse}$) and 1.55 eV ($2 \mu\text{J}/\text{cm}^2/\text{pulse}$), respectively.
- ¹⁴B. Koopmans, M. van Kampen, and W. J. M. de Jonge, *J. Phys.: Condens. Matter* **15**, S723 (2003).
- ¹⁵A. I. Lobad, A. J. Taylor, C. Kwon, S. A. Trugman, and T. R. Gosnell, *Chem. Phys.* **251**, 227 (2000); A. I. Lobad, R. D. Averitt, and A. J. Taylor, *Phys. Rev. B* **63**, 060410(R) (2001); R. D. Averitt, A. I. Lobad, C. Kwon, S. A. Trugman, V. K. Thorsmølle, and A. J. Taylor, *Phys. Rev. Lett.* **87**, 017401 (2001); X. J. Liu, Y. Moritomo, A. Nakamura, H. Tanaka, and T. Kawai, *Phys. Rev. B* **64**, 100401(R) (2001).
- ¹⁶T. Kise, T. Ogasawara, M. Ashida, Y. Tomioka, Y. Tokura, and M. Kuwata-Gonokami, *Phys. Rev. Lett.* **85**, 1986 (2000).
- ¹⁷E. Kojima, R. Shimano, Y. Hashimoto, S. Katsumoto, Y. Iye, and M. Kuwata-Gonokami, *Phys. Rev. B* **68**, 193203 (2003).
- ¹⁸B. Koopmans, M. van Kampen, J. T. Kohlhepp, and W. J. M. de Jonge, *Phys. Rev. Lett.* **85**, 844 (2000).
- ¹⁹L. Guidoni, E. Beaurepaire, and J.-Y. Bigot, *Phys. Rev. Lett.* **89**, 017401 (2002).
- ²⁰K. Matsuda, A. Machida, Y. Moritomo, and A. Nakamura, *Phys. Rev. B* **58**, R4203 (1998); Y. H. Ren, H. B. Zhao, G. Lüpke, Y. F. Hu, and Qi Li, *J. Appl. Phys.* **91**, 7514 (2002).
- ²¹P. Dai, J. A. Fernandez-Baca, N. Wakabayashi, E. W. Plummer, Y. Tomioka, and Y. Tokura, *Phys. Rev. Lett.* **85**, 2553 (2000).
- ²²J. M. De Teresa, M. R. Ibarra, J. Blasco, J. García, C. Marquina, P. A. Algarabel, Z. Arnold, K. Kamenev, C. Ritter, and R. von Helmolt, *Phys. Rev. B* **54**, 1187 (1996); J. M. De Teresa, M. R. Ibarra, P. A. Algarabel, C. Ritter, C. Marquina, J. Blasco, J. García, A. del Moral, and Z. Arnold, *Nature (London)* **386**, 256 (1997).
- ²³T. Dietl, P. Peyla, W. Grieshaber, and Y. Merle d'Aubigné, *Phys. Rev. Lett.* **74**, 474 (1995).
- ²⁴V. A. Atsarkin, V. V. Demidov, G. A. Vasneva, and K. Conder, *Phys. Rev. B* **63**, 092405 (2001).
- ²⁵J. M. De Teresa, M. R. Ibarra, P. Algarabel, L. Morellon, B. García-Landa, C. Marquina, C. Ritter, A. Maignan, C. Martin, B. Raveau, A. Kurbakov, and V. Trounov, *Phys. Rev. B* **65**, 100403(R) (2002).
- ²⁶K. H. Kim, M. Uehara, and S.-W. Cheong, *Phys. Rev. B* **62**, R11 945 (2000).
- ²⁷G. Ju, J. Hohlfield, B. Bergman, R. J. M. van de Veerdonk, O. N. Mryasov, J.-Y. Kim, X. Wu, D. Weller, and B. Koopmans, *Phys. Rev. Lett.* **93**, 197403 (2004).